Three-Dimensional RF MEMS Switch for Power Applications

Joo-Young Choi, Jinyu Ruan, *Student Member, IEEE*, Fabio Coccetti, *Member, IEEE*, and Stepan Lucyszyn, *Senior Member, IEEE*

***Abstract*—This paper introduces a new concept in 3-D RF microelectromechanical systems switches intended for power applications. The novel switch architecture employs electrothermal hydraulic microactuators to provide mechanical actuation and 3-D out-of-plane silicon cantilevers that have both spring action and latching mechanisms. This facilitates an OFF-state gap separation distance of 200 μm between ohmic contacts, without the need for any hold power. Having a simple assembly, many of the inherent problems associated with the more traditional suspension-bridge and cantilever-type-beam architectures can be overcome. A single-pole single-throw switch has been investigated, and its measured ON-state insertion and return losses are less than 0.3 dB up to 10 GHz and greater than 15 dB up to 12 GHz, respectively, while the OFF-state isolation is better than 30 dB up to 12 GHz. The switch works well in both hot- and cold-switching modes, with 4.6 W of RF power at 10 GHz and without any signs of degradation to the ohmic contacts.**

***Index Terms*—Electrothermal hydraulic microactuator, high power, paraffin wax, RF microelectromechanical systems (MEMS), silicon cantilever, switch.**

I. Introduction

THE RF MICROELECTROMECHANICAL systems (MEMS) switches offer many advantages over their solid-state counterparts, in terms of low loss, high isolation, low power consumption, and high linearity [1]. However, RF MEMS switches have reliability issues that can be linked to the RF power level. Generally, RF MEMS switches are based on designs that employ electrostatic actuation, which have various methods for realizing their electrodes. These switches are classified as either capacitive-membrane or metal-to-metal ohmic contact switches [2], [3]. The capacitive-membrane switches have large contact areas, separated by a very thin dielectric layer. The metal-to-metal ohmic contact switches can have relatively small contact areas. In terms of mechanical structure, traditional RF MEMS switches can be divided into those that have architectures based on either suspension bridge or cantilever beams [2]. With the suspension-bridge structure, there are two physical anchors at each end of a beam. In contrast, the cantilever beam only has one anchor, and the other end is free to move.

TABLE I
Comparative Summary of RF MEMS Power Switch Performance

Reference [#]	RF Power (W)	Frequency (GHz)	Switching mode
Peroulis *et al.* [5]	0.8	10	Hot & Cold
Grenier *et al.* [6]	8	10	Cold
McErlean *et al.* [9]	2.3	10	Cold
Palegol *et at.* [12]	1	10	Hot & Cold
	5	3	Hot & Cold
Kwon *et al.* [16]	1.4	2	Cold
Our Work	4.6	10	Hot & Cold

Traditional RF MEMS switches have inherent limitations dictated by RF power handling (e.g., with a failure mechanism due to self-actuation, stiction, electromigration, microscopic bonding, etc.). These problems can be exacerbated by the beam structure employed, which is usually very thin (typically 0.5–2 μm) and has very small gap separation distances between the electrodes (typically 1–5 μm). Considering that the RF power-handling capacity varies between architectural designs, there have been a number of diverse approaches to improve the RF power-handling capacity, for example, the addition of an electrode to pull the beam upward [4]–[6] or to toggle the cantilever beam downward [7]; an array of many switching elements, in order to increase isolation and reduce current density [8], [9]; an increase in the width and thickness of the beam [8], [10]; an increase in the contact force [11]–[13]; and the use of extraordinary contact materials, such as a diamond film [14], [15], Pt, or Ir [16]. A comparative summary of RF MEMS power switch performances is shown in Table I.

Traditional in-plane beam architectures are not ideal for RF MEMS power switch applications. As a result, nonbeam architectures for high-power RF MEMS switches have been investigated. Examples include a ridge waveguide that is integrated with thermally plastic deformable actuators [17] and a water-based absorptive switch [18].

Manuscript received April 17, 2008; revised October 28, 2008. First published December 2, 2008; current version published April 1, 2009. This work was supported in part by Roke Manor Research Ltd. (U.K.) and in part by the European Union's Network of Excellence AMICOM under Contract FP6-507352. In addition, this work was supported by the U.K.'s Engineering and Physical Sciences Research Council (EPSRC) under Platform Grant EP/E063500/1.

J.-Y. Choi is with the Optical and Semiconductor Devices Group, Department of Electrical and Electronic Engineering, Imperial College London, London, SW7 2AZ, U.K.

J. Ruan and F. Coccetti are with Laboratoire d'Architecture et d'Analyse des Systèmes, Centre National de la Recherche Scientifique, 31077 Toulouse, France.

S. Lucyszyn is with the Optical and Semiconductor Devices Group, Department of Electrical and Electronic Engineering, Imperial College London, London, SW7 2AZ, U.K. (e-mail: stepan@ieee.org).

Color versions of one or more of the figures in this paper are available online at http://ieeexplore.ieee.org.

Digital Object Identifier 10.1109/TIE.2008.2010087

0278-0046/$25.00 © 2009 IEEE

Authorized licensed use limited to: Imperial College London. Downloaded on October 20, 2009 at 16:25 from IEEE Xplore. Restrictions apply.

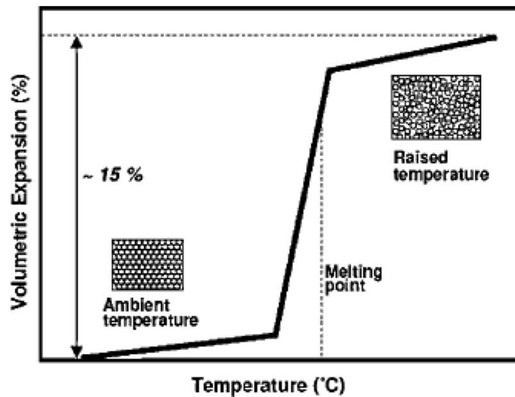

Fig. 1. Expansion characteristics of paraffin wax [19].

Using a previously established electrothermal hydraulic microactuator technology [19]–[21], a very new concept in RF MEMS switch development was briefly introduced [22]. Traditional designs rely on multiple layers of relatively thin conducting, dielectric, and sacrificial materials that have to be surface micromachined. This approach can be very problematic, even for low-power applications, due to poor tolerances in thickness and unwanted built-in stresses. This adds to the difficulty and complexity associated with fabrication processing. By comparison, each part of our switch can be fabricated using simple bulk micromachining and can be easily assembled by gluing. Moreover, the whole fabrication time can be reduced if each part is fabricated in parallel.

For the first time, this paper describes a fully working prototype switch, having totally different cantilever, ohmic contact, and self-assembly designs, to give vastly superior measured performances. Here, mechanical analysis, the introduction of trench/tilted angle structures, and RF power measurement are described. This new approach represents a paradigm shift in the way RF MEMS switches can be implemented, with a view of overcoming the RF power limitations associated with traditional beam-based architectures that employ electrostatic methods of actuation.

II. Concept and Structure

A. Characteristics of Paraffin Wax

Phase-change material (PCM) characteristics can be exploited to realize electrothermal hydraulic microactuators. As a PCM, paraffin wax shows a volumetric expansion of ~15% when it melts and shrinks back to the initial volume on cooling, as shown in Fig. 1. This technology has previously been investigated and employed within a number of non-RF MEMS application demonstrators [19]–[21]. It can also be extended to RF MEMS applications to replace the conventional electrostatic actuation mechanism [22].

B. Switch Concept

The proposed single-pole single-throw switch consists of two paraffin-wax microactuators and silicon cantilevers, as shown in Fig. 2. Instead of simple beams, relatively thick silicon cantilevers (having springs and latches) make an ohmic contact with the coplanar waveguide (CPW) transmission line's signal track. Paraffin-wax microactuators control the silicon cantilevers by means of a mechanical push-and-release mechanism. This simple latching mechanism can maintain both OFF- and ON-states, without continuous dc biasing of any of the microactuators.

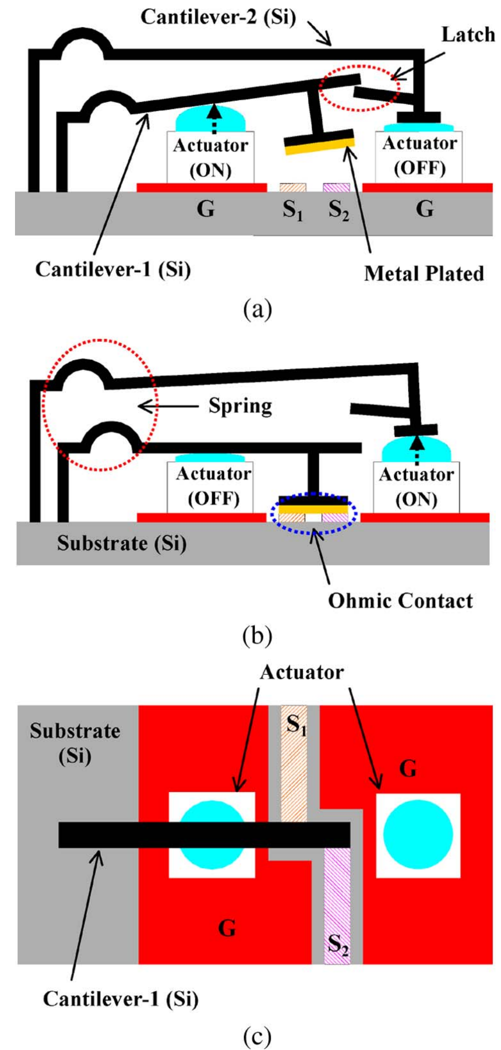

Fig. 2. Basic cross section and top views of the novel RF MEMS switch. (a) OFF-state. (b) ON-state. (c) Top view (without cantilever-2).

C. Microactuators

Within the RF MEMS switch, the associated microactuator consists of paraffin-wax containers and thick silicon cantilevers. With the former, the microactuator technology has already been described in detail [19]–[21] for non-RF MEMS applications. The structure of the container is shown in Fig. 3. Paraffin wax fills the bulk-micromachined silicon containers, which are sealed using an elastic diaphragm of polydimethylsiloxane (PDMS). When the required dc bias voltage is applied to the integrated microheater, the paraffin wax expands with the associated increase in heat and is then deliberately shaped into a hemisphere.

With the latter, silicon cantilevers are inspired from elements from a microgripper [20]. Two silicon cantilevers are

Authorized licensed use limited to: Imperial College London. Downloaded on October 20, 2009 at 16:25 from IEEE Xplore. Restrictions apply.

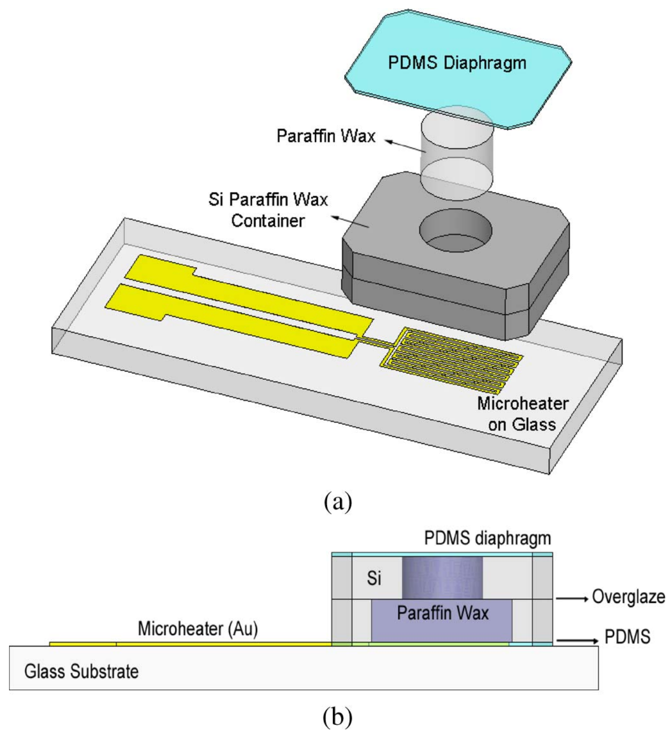

(a)

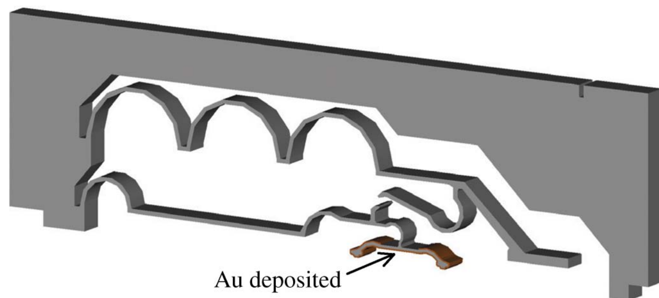

(b)

Fig. 3. Electrothermal hydraulic microactuator. (a) Exploded view. (b) Cross-sectional view.

Fig. 4. Designed silicon cantilever with springs and latches.

employed—one for the ohmic contacts and the other for the latching mechanism. With the former, gold is selectively deposited onto the cantilever pins, in order to provide a metal-to-metal ohmic contact with the CPW's signal lines (S1 and S2 in Fig. 2). Fig. 4 shows the cantilever elements and latching mechanisms integrated into one piece of silicon, to simplify assembly. With the most common silicon wafer thickness of $\sim$525 μm, wide ohmic contacts can be created for RF power applications when compared with conventional switches that may have contact areas on the order of 10×10 μm^2. Moreover, these microactuators can introduce OFF-state gap separation distances greater than 200 μm, in order to enhance the OFF-state RF isolation characteristics.

D. Assembly and Ohmic Contacts

The paraffin-wax microactuators only offer an expansion force that can lift up the cantilever beams. Therefore, it can be difficult to achieve a constant ohmic contact pressure. As a result, the beam was redesigned to have a tilted angle below the horizontal level, in order to provide a spring force between the cantilever and the CPW lines after assembly, as shown in Fig. 5.

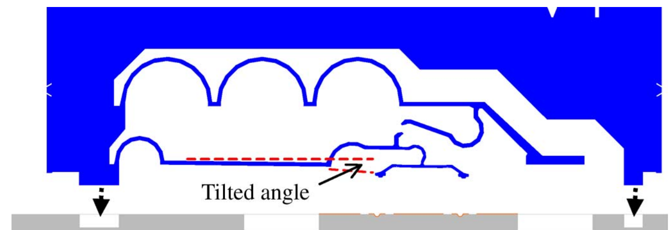

Fig. 5. Beam structure having a tilted angle.

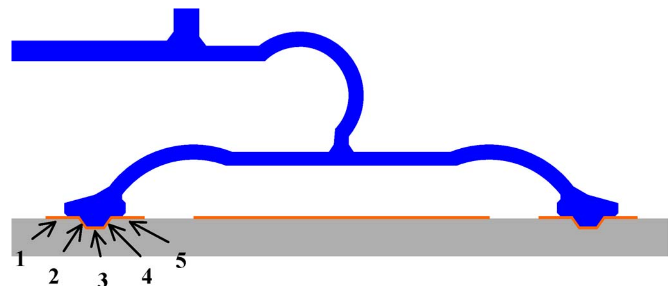

Fig. 6. Illustration of the self-aligned trench structure showing each contact pin having five ohmic contact surfaces.

In addition to the tilted beam, trenches in the bottom silicon substrate were introduced for the first time, where the cantilever pins make contact with the CPW's signal lines. Each contact pin has five contact surfaces, as shown in Fig. 6. The contact area is 0.14 mm^2, which represents an increase of 20% using this trench structure, when compared when the first experimental switch [22]. Considering the dependence of the contact resistance on the size of the contact area, the mechanical force, and the quality of the contact [1], [23], the trenches can reduce the ohmic contact resistance by increasing the contact area and, thus, minimize heat dissipated in the surrounding area. Enhanced RF power handling can therefore be expected, which lowers the temperature at the contact area [24]–[26] and reduces the failure due to electromigration and microscopic bonding. Moreover, the use of a trench effectively creates a self-aligned structure.

III. SIMULATIONS

Extensive iterative optimizations between mechanical and RF operations were carried out. A summary of each individual procedure will be described in this section.

A. Mechanical Characteristics

The relatively complex mechanical mechanisms were investigated using commercial computer-aided design software. Here, *ANSYS (V9.0)* was used for both the alignment of the cantilever pins to the trenches and the latching mechanism. Fig. 7 shows *ANSYS* simulation results.

Despite the effect of contact force on the contact resistance, the contact force had to be limited so that the expansion of paraffin wax pushing on the silicon cantilever can achieve the

Authorized licensed use limited to: Imperial College London. Downloaded on October 20, 2009 at 16:25 from IEEE Xplore. Restrictions apply.

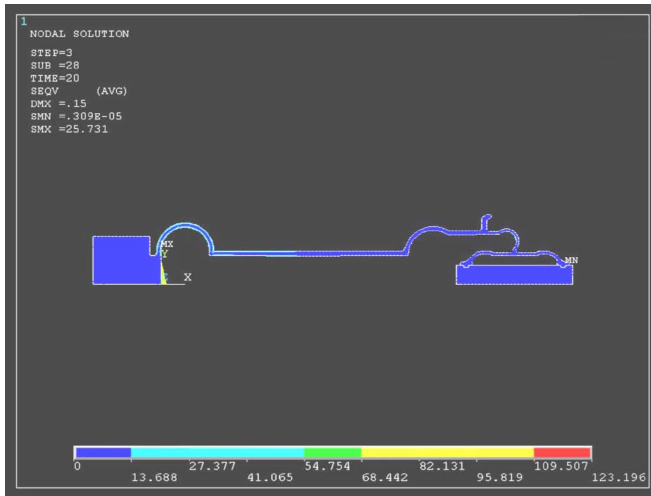

(a)

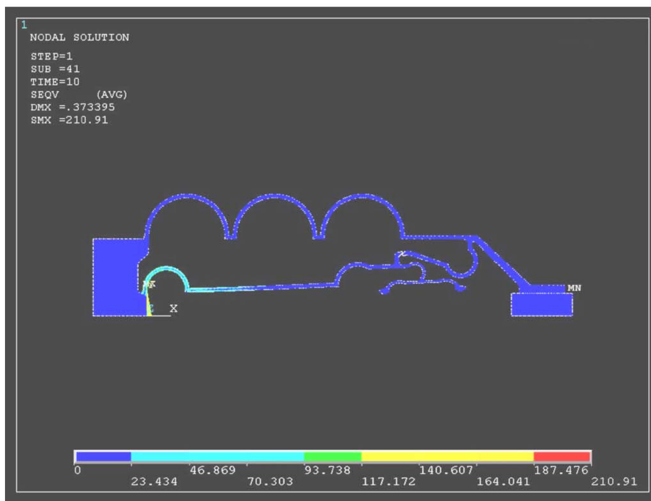

(b)

Fig. 7. Silicon cantilever design using *ANSYS*. (a) Simulations of alignment to the trenches. (b) Simulations of latching mechanism (unit of stress: megapascals).

200-μm target separation distance. If the contact force is too high (due to a large tilt angle, stiff cantilever, short beam length, etc.), the silicon cantilever cannot be lifted as high as intended. Based on previous research on pressure from the actuator [20], the tilt angle was designed to be 0.6°, in order to provide ∼5 mN of contact force, which is 20 times greater than that of typical conventional beam structures [1]. The yield stress also has to be considered. The maximum stress on the silicon cantilever is approximately 0.21 GPa, which is less than the yield stress of silicon (7 GPa) [27].

B. RF Characteristics

The RF characteristics of the switch with CPW lines, including trench features and the silicon cantilever designed using ANSYS, need to be verified. If the mechanically optimized cantilever structure does not give suitable RF performance, the design has to be modified. Considering the size and location of the paraffin-wax containers, trenches, and RF probes (for measurements), CPW lines on the bottom substrate were designed as shown in Fig. 8. The final simulation results up to Ku-band from CPW lines and 3-D models, using a high-frequency structural simulator (HFSS$^{\text{TM}}$), are shown in Fig. 9.

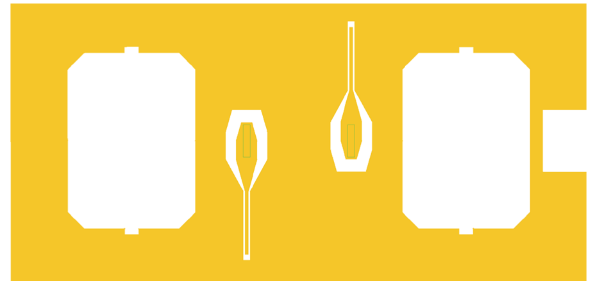

Fig. 8. Top view illustrating the CPW lines on the bottom substrate.

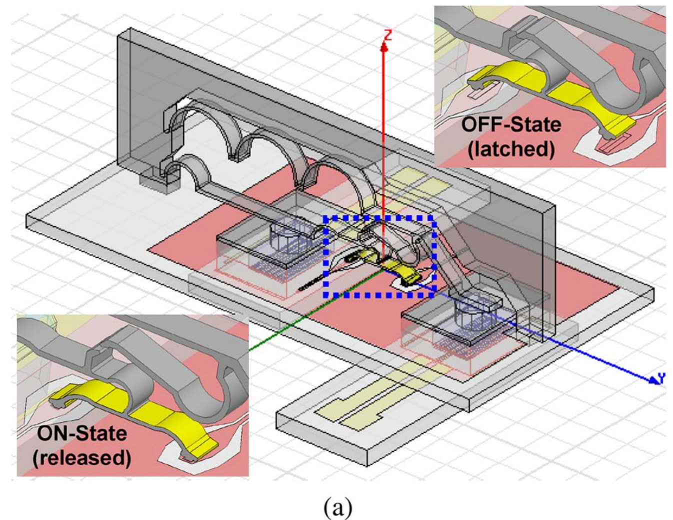

(a)

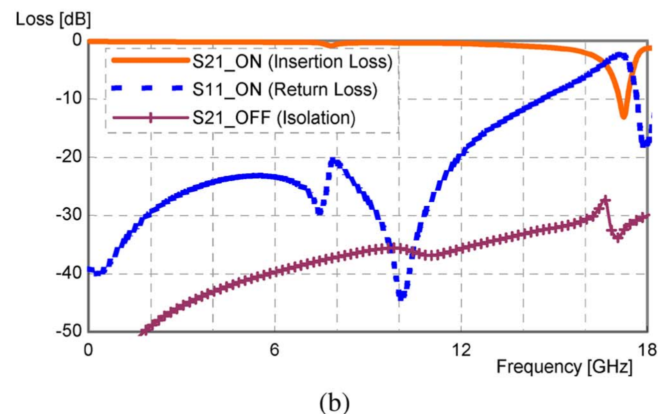

(b)

Fig. 9. Simulated RF performance using *HFSS*$^{\text{TM}}$. (a) Three-dimensional model. (b) Predicted insertion and return losses for ON-state and isolation for OFF-state.

It can be seen that the predicted worst case ON-state insertion and return loss levels up to 14 GHz are 1 and 12 dB, respectively, and the minimum OFF-state isolation is 33 dB. It should be noted that the insertion loss values include the loss from feed lines, considering that unlike the wave port configuration, direct deembedding is not applicable with the lumped port configuration used within these simulations.

The lever pins and a section of the associated silicon cantilever are coated with gold. This acts as an open-circuit

Authorized licensed use limited to: Imperial College London. Downloaded on October 20, 2009 at 16:25 from IEEE Xplore. Restrictions apply.

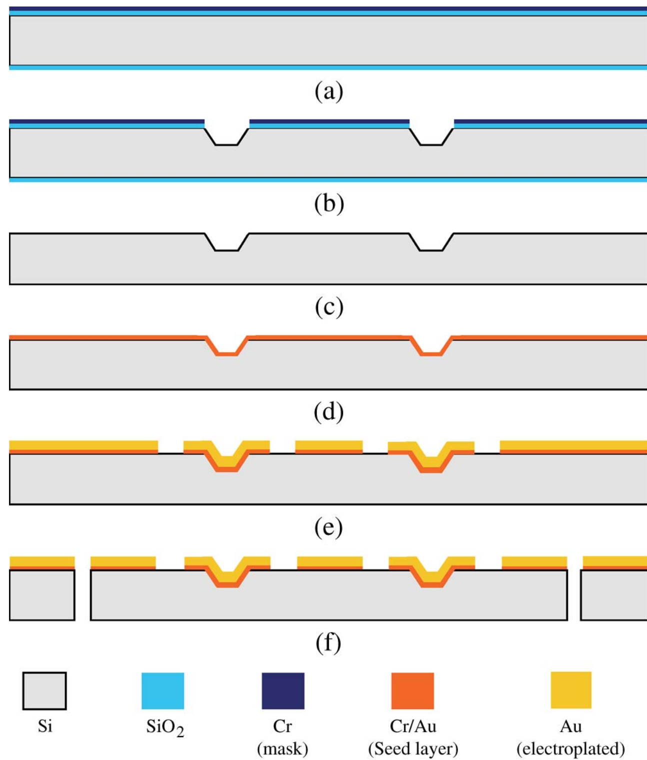

Fig. 10. Fabrication process flow for the main substrate. (a) Mask for KOH etching: thermal oxidation and sputtering of Cr. (b) KOH etching: photolithography; Cr etching, SiO_2 etching and Si etching (KOH etching). (c) SiO_2 layer removal: Cr mask removal and SiO_2 removal (both sides). (d) Seed layer deposition: sputtering of Cr/Au seed layer. (e) Au patterning: photolithography, Au electroplating and seed layer etching. (f) Separation of each substrate: photolithography and deep reactive-ion etching (DRIE).

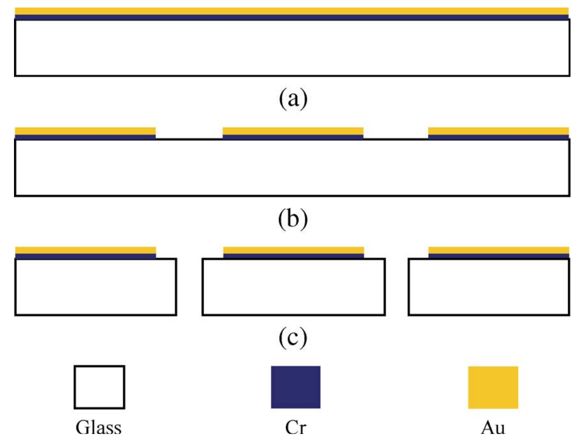

Fig. 11. Fabrication process flow for the microheaters. (a) Metal layer deposition: sputtering of Cr and Au layers. (b) Au patterning: photolithography and Cr and Au etching. (c) Dicing.

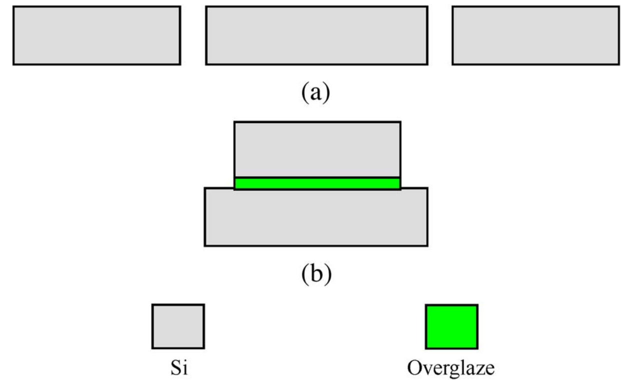

Fig. 12. Fabrication process flow for the paraffin-wax containers. (a) Separation of container pieces: photolithography and DRIE. (b) Buildup of containers: applying overglaze and baking at 550 °C.

resonant stub, with a predicted resonance at around 17 GHz unless corrective action is taken to avoid in-band resonances.

IV. Fabrication

The whole fabrication process consists of silicon bulk micromachining and assembly. Bulk micromachining is divided into four kinds of processing for the different components (i.e., microheaters, paraffin-wax containers, silicon cantilevers, and CPW lines). In addition to microfabrication processing used for the first experimental switch design [22], a potassium hydroxide (KOH) etching process was required to form trench structures within the silicon substrate. Moreover, considering the current density for RF power applications, relatively thick, at $\sim$3 μm, layers of gold were deposited to form the CPW lines and ohmic contact pins. Four process flows (for the main substrates, microheaters, paraffin-wax containers, and silicon cantilevers) are shown in Figs. 10–13, respectively.

The paraffin-wax container is attached to the glass microheater substrate using PDMS, and microactuators are themselves completed by covering the paraffin-wax container with PDMS. The switch is assembled by inserting two microactuators into the main silicon substrate and the cantilever substrate into the predesignated slots within the main substrate, as shown in Fig. 14. Compared with the first experimental switch, where the microactuators were located on top of the main substrate [22], this solution not only exploits the benefits of self-alignment but also reduces the height of the device.

V. Measurement Results

The dc contact resistance was measured to be between 1.5 and 2 Ω. The actual contact area and force can vary with the tolerance of fabrication and assembly. This relatively high contact resistance is believed to result from the rough contact surfaces, due to our thick in-house gold electroplating process. RF measurements of the assembled switches were conducted up to Ku-band. Fig. 15 shows a switch under test using a Cascade Microtech probe station, with the silicon cantilever actuated into the latched OFF-state and released ON-state.

A. RF Characteristics—Small-Signal Measurements

The equivalent circuit models for the switch are shown in Fig. 16. In the ON-state, the series inductance L_{se} represents the gold-plated section of silicon between the cantilever pins, and the shunt capacitance C_{sh} represents the capacitance between the ground and the contact trench pad at the end of the CPW signal line. The contact resistance R_c is placed between the contact trench pad and the cantilever pin. Capacitive coupling between

Authorized licensed use limited to: Imperial College London. Downloaded on October 20, 2009 at 16:25 from IEEE Xplore. Restrictions apply.

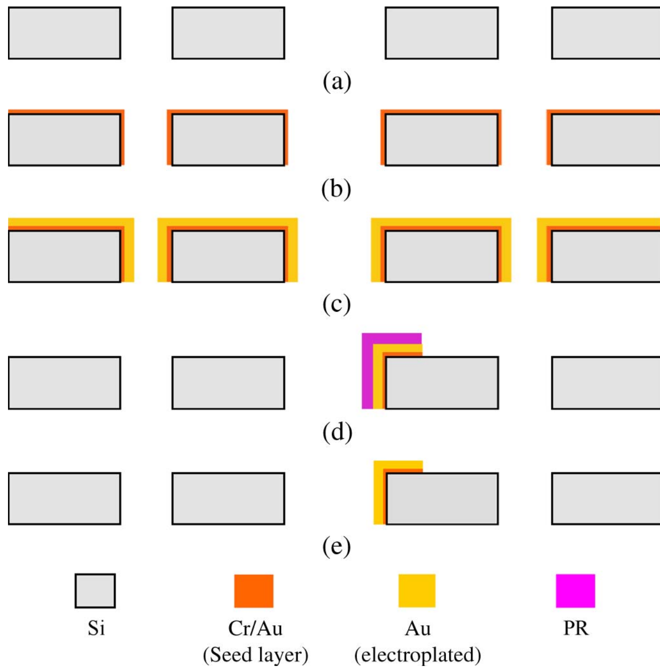

Fig. 13. Fabrication process flow for the silicon cantilevers. (a) Shaping of silicon cantilever structure: photolithography and DRIE. (b) Seed layer deposition: sputtering of Cr/Au seed layer. (c) Au electroplating. (d) Formation of cantilever pins: masking cantilever pins with photoresist (PR) and etching (Au → Cr). (e) PR removal.

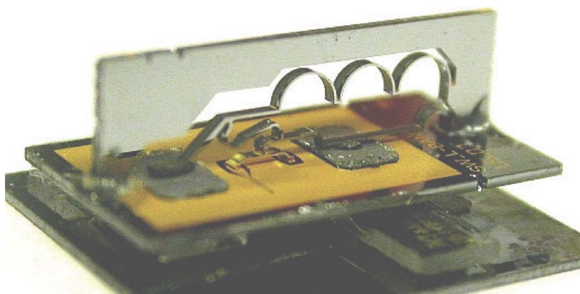

Fig. 14. Assembled switch with main substrate dimensions of $15 \times 7\ \mathrm{mm}^2$.

two contact trench pads is provided by C_c. In addition, the shunt resistance R_b represents the silicon cantilever beam having a high resistivity connected to the main substrate from the center of the pins. In the OFF-state, the contact resistance is replaced with the series capacitance C_{se}, which represents the capacitance between the cantilever pin and the contact trench pad.

Fig. 17 shows the measured ON-state frequency responses of the switch in comparison with electromagnetic simulation results from *HFSS*$^{\mathrm{TM}}$ and equivalent circuit model simulation results (with $L_{se} = 0.33$ nH, $C_c = 0.01$ pF, $R_c = 2\ \Omega$, $C_{sh} = 0.22$ pF, and $R_b = 1.7\ \mathrm{k}\Omega$). There is very good agreement between the electromagnetic and the equivalent circuit model simulation results, which also both follow the measured frequency responses. It is worth mentioning that, as a result of our findings from the previous HFSS$^{\mathrm{TM}}$ simulations, the length of the gold-coated section of the cantilever was limited, thus greatly increasing the lowest resonant frequency. This is why the unwanted resonance in not seen in measurements below 18 GHz.

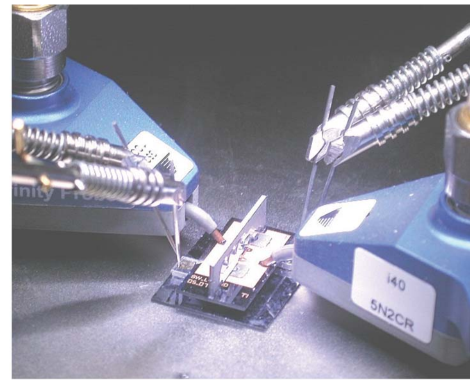

(a)

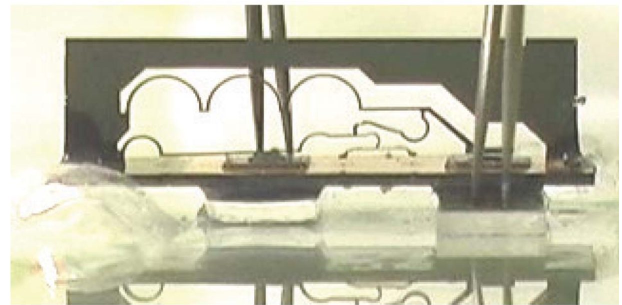

(b)

Fig. 15. Switch testing. (a) On-wafer RF measurements. (b) DC actuation test.

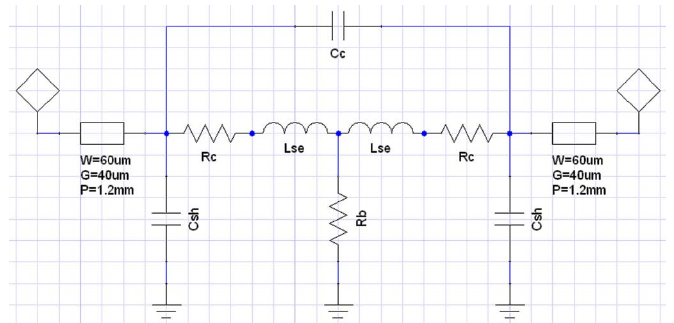

(a)

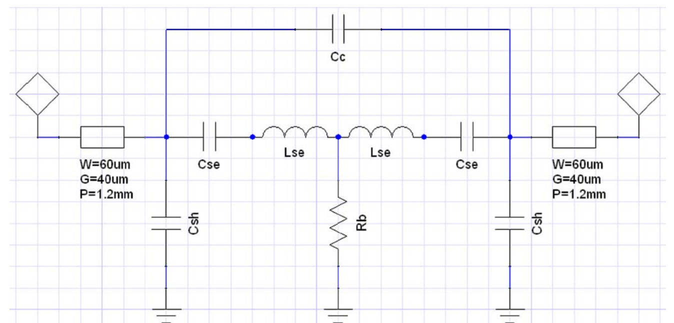

(b)

Fig. 16. Equivalent circuit model for the switch. (a) ON-state. (b) OFF-state.

It can be seen that the measured ON-state insertion loss (I.L.) and return loss (R.L.) without deembedding of feed lines are less than 1 dB and greater than 11 dB, respectively, up to 14 GHz. Taking into account the 0.26-dB feed lines' losses at 10 GHz, as shown in Fig. 18, the insertion loss below 10 GHz is less than 0.3 dB.

Authorized licensed use limited to: Imperial College London. Downloaded on October 20, 2009 at 16:25 from IEEE Xplore. Restrictions apply.

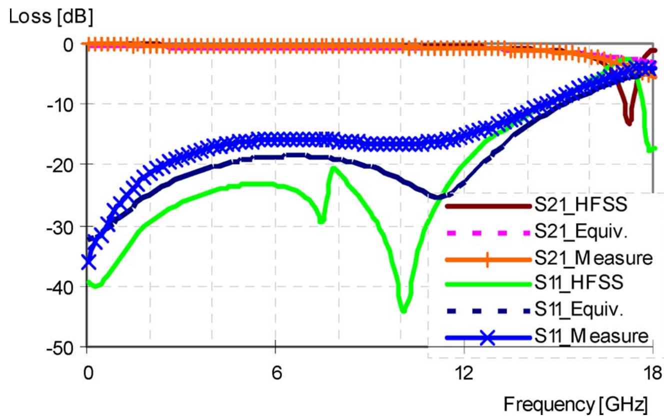

Fig. 17. Measured ON-state frequency responses in comparison with *HFSS*$^{\mathrm{TM}}$ and equivalent circuit model simulation results.

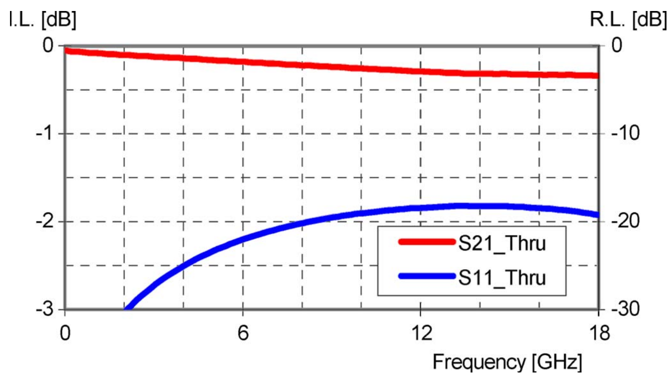

Fig. 18. Measured switch feed line losses.

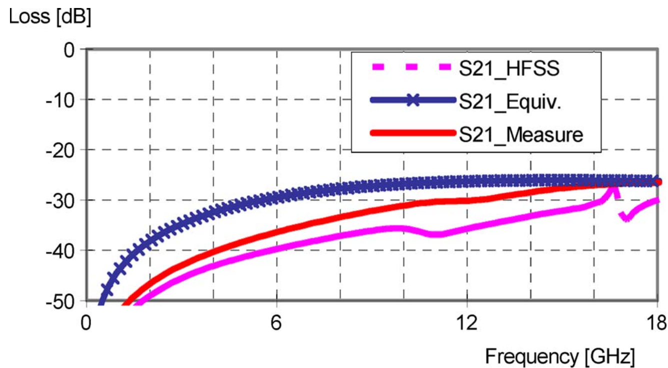

Fig. 19. Measured OFF-state frequency responses in comparison with *HFSS*$^{\mathrm{TM}}$ and equivalent circuit model simulated results.

Fig. 19 shows the measured OFF-state frequency responses of the switch in comparison with simulation results from *HFSS*$^{\mathrm{TM}}$ and equivalent circuit model simulation results (with R_c replaced by $C_{se} = 5$ fF). The measured OFF-state isolation is greater than 27 dB, up to 16 GHz. Once again, there is good agreement between the measured and the modeled frequency responses.

B. RF Characteristics—Power Measurements

To examine the high-RF power-handling capability of the switch, power measurements at 10 GHz were carried out at the Laboratoire d'Architecture et d'Analyse des Systèmes, Centre National de la Recherche Scientifique (Toulouse, France). The measurement setup is shown in Fig. 20. Although the gain of the amplifier was 39 dB, the input RF power to the amplifier was limited to 0 dBm, to avoid saturation. Considering losses from cables and components, the maximum RF power that could reach the device under test (DUT) was only 4.6 W.

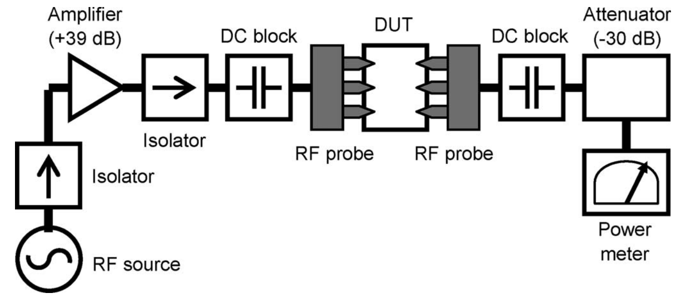

Fig. 20. Measurement setup for high-power testing at 10 GHz.

TABLE II
APPLIED BIAS

States	Voltage (V)	Current (mA)
Latching ON → OFF	11.5	46
Releasing OFF → ON	10.0	48

TABLE III
ACTUATION TIMES

Sample	Latching ON → OFF (seconds)	Releasing OFF → ON (seconds)
1	13	5
2	12	5
3	12	6
4	12	6

The switch was tested in the hot-switching mode for ten cycles, with varying times in the ON-state. Under such conditions, it was found that the switch can operate with 4.6 W of RF power at 10 GHz, without any observable degradation in performance. From Table I, it can be seen that our switch has the highest combined operating frequency and RF power level for both hot- and cold-switching modes. Moreover, we are confident that this unique switch can operate at even higher operating frequencies and RF power levels; however, the facilities to prove this were not available to us at this time.

C. Mechanical Characteristics

The applied bias and actuation times are summarized in Tables II and III, respectively. The microactuator itself can change its phase within 2–3 s; however, it takes longer to reach a power level sufficient to complete latching and subsequent releasing of the beam.

The remainder of the actuation time, approximately 9–11 s, is spent undertaking the actual latching. Assuming the elasticity and deformation of the silicon beam are properly calculated within *ANSYS* simulations, another important factor to be taken into consideration is the friction of the bulk-micromachined silicon surfaces. Considering that two latching parts slide, as shown in Fig. 21, the loading force required from the microactuators will be altered based on the amount of friction.

Authorized licensed use limited to: Imperial College London. Downloaded on October 20, 2009 at 16:25 from IEEE Xplore. Restrictions apply.

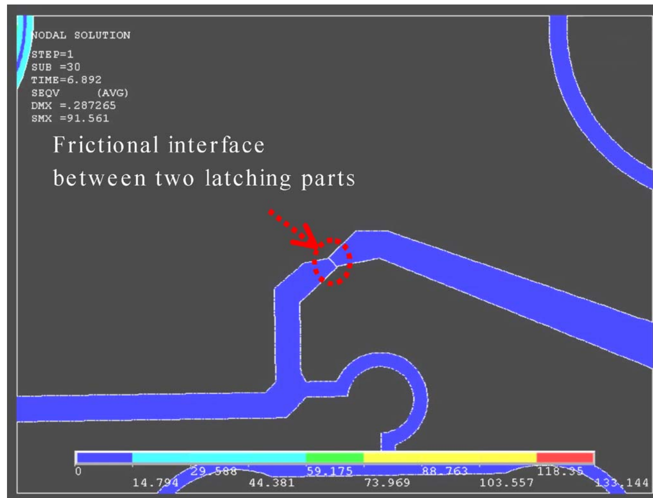

Fig. 21. Loading force simulation results for the latching mechanism.

It can be seen that 500 mW of dc power is consumed by the suboptimal microactuator design. This issue was briefly discussed in [19], where only 300 mW of dc power was required for a similar type of microactuator design. However, with our switch implementation, the dc power is only consumed during the actuation phase, since latching is employed to avoid the need for any hold power in either the ON- or OFF-states. Having said this, there are a number of ways to reduce the dc-power consumption during the switching phase. For example, one could use a paraffin wax that has a lower phase-transition temperature. Moreover, the design of the microheater/wax interface can be optimized. In addition, the latching mechanism can be designed to cater for a reduced volume of paraffin wax.

VI. Conclusion

A novel RF MEMS switch, intended for RF power applications, has been developed. An iterative design process for the switch has been established between *ANSYS* (for the mechanical structural design) and *HFSS*$^{\text{TM}}$ (for the RF design). The switch has a completely unique physical structure, when compared with conventional RF MEMS switches. For example, this 3-D switch employs electrothermal hydraulic microactuators; silicon cantilever mechanisms with spring action and latching mechanism; and bulk-micromachined trenches having five ohmic contact points. When these features are combined into an RF MEMS switch, not only does the switch have an excellent RF performance under small-signal conditions but it is also expected to have advantages with RF power handling beyond 4.6 W at 10 GHz. In addition, there are additional benefits, such as self-alignment during assembly, modular structure, simple dc biasing, and robust operation. However, its inherent large size/mass, low actuation speed, and complex construction make this switch only suitable for niche applications, where good RF power handling is important (e.g., high-power amplifier redundancy).

This design could potentially handle high power, provided that the correct contact metal is used and a proper study is performed to characterize the power handling. As with all new RF MEMS technologies, exhaustive reliability testing under small-signal and high-power conditions is required; however, this is beyond the scope of this paper.

Acknowledgment

The authors would like to thank Dr. M. M. Ahmad, Dr. G. Hong, and Dr. J.-S. Lee for their help during the fabrication processing. The authors would also like to thank Dr. M. Hickson at Roke Manor Research Ltd. (U.K.) for his support.

References

[1] G. M. Rebeiz, *RF MEMS–Theory, Design and Technology*. Hoboken, NJ: Wiley, 2003.
[2] S. Lucyszyn, "Review of radio frequency microelectromechanical systems (RF MEMS) technology," *Proc. Inst. Elect. Eng.—Sci., Meas. Technol.*, vol. 151, no. 2, pp. 93–103, Mar. 2004.
[3] L. P. B. Katehi, J. F. Harvey, and E. Brown, "MEMS and Si micromachined circuits for high-frequency applications," *IEEE Trans. Microw. Theory Tech.*, vol. 50, no. 3, pp. 858–866, Mar. 2002.
[4] K. M. Strohm, B. Schauwecker, D. Pilz, W. Simon, and J.-F. Luy, "RF-MEMS switching concepts for high power applications," in *Proc. Topical Meeting Silicon Monolithic Integr. Circuits RF Syst.*, Ann Arbor, MI, Sep. 2001, pp. 42–46.
[5] D. Peroulis, S. P. Pacheco, and L. P. B. Katehi, "RF MEMS switches with enhanced power-handling capabilities," *IEEE Trans. Microw. Theory Tech.*, vol. 52, no. 1, pp. 59–68, Jan. 2004.
[6] K. Grenier, D. Dubuc, B. Ducarouge, V. Conedera, D. Bourrier, E. Ongareau, P. Derderian, and R. Plana, "High power handling RF MEMS design and technology," in *Proc. 18th IEEE Int. Conf. MEMS*, Miami, FL, Jan. 30–Feb. 3 2005, pp. 155–158.
[7] W. Simon, B. Schauwecker, A. Lauer, and A. Wien, "Designing a novel RF MEMS switch for broadband power applications," in *Proc. Eur. Microw. Conf.*, Milan, Italy, Sep. 2002, pp. 519–522.
[8] N. Nishijima, J.-J. Hung, and G. M. Rebeiz, "Parallel-contact metal-contact RF-MEMS switches for high power applications," in *Proc. 17th IEEE Int. Conf. Micro Electro Mechanical Syst.*, Maastricht, The Netherlands, Jan. 2004, pp. 781–784.
[9] E. P. McErlean, J.-S. Hong, S. G. Tan, L. Wang, Z. Cui, R. B. Greed, and D. C. Voyce, "2 × 2 RF MEMS switch matrix," *Proc. Inst. Elect. Eng.—Microw., Antennas Propag.*, vol. 152, no. 6, pp. 449–454, Dec. 9, 2005.
[10] L. L. W. Chow, Z. Wang, B. D. Jensen, K. Saitou, J. L. Volakis, and K. Kurabayashi, "Skin effect aggregated heating in RF MEMS suspended structures," in *IEEE MTT-S Int. Microw. Symp. Tech. Dig.*, Jun. 12–17, 2005, pp. 2143–2146.
[11] B. D. Jensen, L. W. Chow, R. F. Webbink, K. Saitou, J. L. Volakis, and K. Kurabayashi, "Force dependence of RF MEMS switch contact heating," in *Proc. 17th IEEE Int. Conf. MEMS*, 2004, pp. 137–140.
[12] C. Palegol, A. Pothierl, T. Gasseling, A. Crunteanul, C. Cibert, C. Champeaux, P. Tristant, A. Catherinot, and P. Blondy, "RF-MEMS switched varactor for high power applications," in *IEEE MTT-S Int. Microw. Symp. Tech. Dig.*, Jun. 2006, vol. 1, pp. 35–38.
[13] C. Siegel, V. Ziegler, B. Schönlinner, U. Prechtel, and H. Schumacher, "Simplified RF-MEMS switches using implanted conductors and thermal oxide," in *Proc. 36th Eur. Microw. Conf.*, Manchester, U.K., Sep. 2006, pp. 1735–1738.
[14] E. Kohn, W. Menzel, F. J. Hernandez-Guillen, A. Munding, P. Scgmid, D. Grobe, and J. Kusterer, "Evaluation of CVD diamond for heavy duty microwave switches," in *IEEE MTT-S Tech. Dig.*, 2003, vol. 3, pp. 1625–1628.
[15] E. Kohn, J. Kusterer, and A. Denisenko, "Diamond for high power electronics," in *IEEE MTT-S Int. Microw. Symp. Tech. Dig.*, Jun. 12–17, 2005, pp. 901–904.
[16] H. Kwon, D.-J. Choi, J.-H. Park, H.-C. Lee, Y.-H. Park, Y.-D. Kim, H.-J. Nam, Y.-C. Joo, and J.-U. Bu, "Contact materials and reliability for high power RF-MEMS switches," in *Proc. IEEE 20th Int. Conf. Micro Electro Mech. Syst.*, Jan. 21–25, 2007, pp. 231–234.
[17] M. Daneshmand, R. R. Mansour, and N. Sarkar, "RF MEMS waveguide switch," in *IEEE MTT-S Int. Microw. Symp. Tech. Dig.*, Jun. 6–11, 2004, vol. 2, pp. 589–592.

Authorized licensed use limited to: Imperial College London. Downloaded on October 20, 2009 at 16:25 from IEEE Xplore. Restrictions apply.

[18] C.-H. Chen and D. Peroulis, "Liquid RF MEMS wideband reflective and absorptive switches," *IEEE Trans. Microw. Theory Tech.*, vol. 55, pt. 2, no. 12, pp. 2919–2929, Dec. 2007.
[19] J. S. Lee and S. Lucyszyn, "A micromachined refreshable Braille cell," *J. Microelectromech. Syst.*, vol. 14, no. 4, pp. 673–682, Aug. 2005.
[20] J. S. Lee and S. Lucyszyn, "Design and pressure analysis for bulk-micromachined electrothermal hydraulic microactuators using a PCM," *Sens. Actuators A, Phys.*, vol. 133, no. 2, pp. 294–300, Feb. 2007.
[21] J. S. Lee and S. Lucyszyn, "Thermal analysis for bulk-micromachined electrothermal hydraulic microactuators using a phase change material," *Sens. Actuators A, Phys.*, vol. 135, no. 2, pp. 731–739, Apr. 2007.
[22] J.-Y. Choi, J.-S. Lee, and S. Lucyszyn, "Development of RF MEMS switches for high power applications," in *Proc. IEEE MMS*, Genoa, Italy, Sep. 2006, pp. 294–297.
[23] D. Hyman and M. Mehregany, "Contact physics of gold microcontacts for MEMS switches," *IEEE Trans. Microw. Theory Tech.*, vol. 22, no. 3, pp. 357–364, Sep. 1999.
[24] B. D. Jensen, K. Saitou, J. L. Volakis, and K. Kurabayashi, "Fully integrated electrothermal multidomain modeling of RF MEMS switches," *IEEE Microw. Wireless Compon. Lett.*, vol. 13, no. 9, pp. 364–366, Sep. 2003.
[25] B. Ivira, R.-Y. Fillit, F. Ndagijimana, P. Benech, G. Parat, and P. Ancey, "Self-heating study of bulk acoustic wave resonators under high RF power," *IEEE Trans. Ultrason., Ferroelectr., Freq. Control*, vol. 55, no. 1, pp. 139–147, Jan. 2008.
[26] L. L. Mercado, T. Lee, S.-M. Kuo, V. Hause, and C. Amrine, "Thermal solutions for discrete and wafer-level RF MEMS switch packages," *IEEE Trans. Adv. Packag.*, vol. 26, no. 3, pp. 318–326, Aug. 2003.
[27] M. J. Madou, *Fundamentals of Microfabrication*, 2nd ed. Boca Raton, FL: CRC Press, 2002.

Joo-Young Choi was born in Korea, in 1973. He received the B.Sc. and M.Sc. degrees in electronic engineering from Sogang University, Seoul, Korea, in 1996 and 1998, respectively. He has been working toward the Ph.D. degree in the Optical and Semiconductor Devices Group, Department of Electrical and Electronic Engineering, Imperial College London, London, U.K., since October 2004.

From 1998 to 2004, he was with Samsung Electro-Mechanics, Suwon, Korea, as a Full-Time Researcher, where he developed monoblock duplexers for code-division multiple-access mobile phones and multiband antenna switch modules and front-end modules, using low-temperature cofired ceramic technology for global systems for mobile phones. His current research interests include millimeter-wave filters and microelectromechanical systems devices.

Jinyu Ruan (S'07) was born in Guang Dong, China, and grew up in French Guiana. He received the B.S. degree in electronics, electrical engineering, and automation and the M.S. degree in electrical engineering for high-frequency telecommunication systems from the University of Marne la Vallée, Paris, France, in 2006. He is currently working toward the Ph.D. degree in the Laboratoire d'Architecture et d'Analyse des Systèmes, Centre National de la Recherche Scientifique, Toulouse, France, where his Ph.D. studies are supported by several research projects involved in the reliability of RF microelectromechanical systems (MEMS), including design modeling and testing.

Before working toward the Ph.D. degree, he did six months' training on the fabrication of photodetectors using silicon with MEMS technology processes. His main research interest is the electrical characterization of RF MEMS, particularly dielectric charging effects and electrostatic discharge failures.

Fabio Coccetti (S'98–M'06) received the Laurea (M.S.) degree in electrical engineering from the University of Perugia, Perugia, Italy, in 1999, and the Ph.D. degree in high-frequency engineering from the Lehrstuhl für Hochfrequenztechnik, Technische Universität München, Munich, Germany, in 2004.

For seven months, in 2000, he was a Visiting Scientist with the Radiation Laboratory, University of Michigan, Ann Arbor. During the period 2001–2002, he joined a number of R&D projects with German companies (BOSCH, Siemens, and Rohde & Schwarz) and the European Space Agency in the area of RF microelectromechanical systems (MEMS)-based circuits. Since September 2004, he has been a Research Scientist with the Laboratoire d'Architecture et d'Analyse des Systèmes, Centre National de la Recherche Scientifique, Toulouse, France, where he has been working on numerous research projects, including design modeling, theoretical investigation, and experimental validation and testing of power handling for RF MEMS devices. His research interests include numerical technique optimization; multiphysics and reliability analysis of RF MEMS components; and design and modeling of reconfigurable circuits for microwave and millimeter applications.

Dr. Coccetti is a member of the European Microwave Association and is one of the five cofounders of the European Forum of Experts on RF MEMS and RF microsystem technology. From 2004 to 2007, he was the Coordinator of the European Network of Excellence on RF MEMS and RF microsystems and a member of the ARRRO consortium (both projects funded by the European Commission under the 6th Framework Program).

Stepan Lucyszyn (M'91–SM'04) received the B.S. degree from the Polytechnic of North London, London, U.K., in 1987, the M.S. degree from the University of Surrey, Guildford, U.K., in 1988, and the Ph.D. degree from King's College, University of London, London, in 1992.

He is currently an Associate Professor of millimeter-wave electronics with the Optical and Semiconductor Device Group, Department of Electrical and Electronic Engineering, Imperial College London, London, U.K., and a Visiting Professor with Tsinghua University, Beijing, China. Following 12 years of RFIC/monolithic microwave integrated circuit research, he has spent the past eight years focusing on RF microelectromechanical systems (MEMSs). In 1999, he was a Tan Chin Tuan Exchange Fellow in Engineering with Nanyang Technological University, Singapore. During the summer of 2002, he was a Guest Researcher with the MEMS Laboratory, National Institute of Advanced Industrial Science and Technology, Tsukuba, Japan. To date, he has (co)authored well over 100 technical papers on applied physics and engineering, and presented many invited lectures at international conferences and workshops. Over the past few years, he has been an External Examiner for numerous research students in the U.K., Singapore, and China. In addition, he has sat on European panels for the funding of research projects and served as a member of technical program committees for international conferences.

Dr. Lucyszyn was the recipient of an Institution of Electrical Engineers (IEE) Premium Award in 2005 for a review paper, which he published in 2004, on RF MEMS technology. From 2004 to 2007, he represented Imperial within the European Union's Framework VI Network of Excellence on Advanced MEMS for RF and Millimeter Wave Communications. In November 2005, he was appointed as an Associate Editor for the JOURNAL OF MICROELECTROMECHANICAL SYSTEMS. In 2005, he was elected a Fellow of the IEE (U.K.) and Fellow of the Institute of Physics (U.K.) and, in 2008, was made a Fellow of the Electromagnetics Academy (USA).

Authorized licensed use limited to: Imperial College London. Downloaded on October 20, 2009 at 16:25 from IEEE Xplore. Restrictions apply.